VEGF counteracts shear stress-determined arterial fate specification during capillary remodeling.

Dongying Chen[1,*], Oleksii S. Rukhlenko[2], Brian G. Coon[1,#], Divyesh Joshi[1], Raja Chakraborty[1], Kathleen A. Martin[1], Boris N. Kholodenko[2,3,4], Martin A. Schwartz[1,5,6,*], Michael Simons[1,5,*]

[1] Yale Cardiovascular Research Center, Department of Internal Medicine, Yale University School of Medicine, New Haven, United States.
[2] Systems Biology Ireland, School of Medicine, University College Dublin, Dublin, Ireland.
[3] Conway Institute of Biomolecular & Biomedical Research, University College Dublin, Dublin, Ireland
[4] Department of Pharmacology, Yale University School of Medicine, New Haven, United States.
[5] Department of Cell Biology, Yale University School of Medicine, New Haven, CT, United States.
[6] Department of Biomedical Engineering, Yale University, New Haven, CT, United States.
[#] Current address: Cardiovascular Biology Research Program, Oklahoma Medical Research Foundation, Oklahoma City, United States

* Corresponding authors:
Dongying Chen: dongying.chen@yale.edu
Martin A. Schwartz: martin.schwartz@yale.edu
Michael Simons: michael.simons@yale.edu

Abstract

A key feature of arteriogenesis is capillary-to-arterial endothelial cell fate transition. Although a number of studies in the past two decades suggested this process is driven by VEGF activation of Notch signaling, how arteriogenesis is regulated remains poorly understood. Here we report that arterial specification is mediated by fluid shear stress (FSS) independent of VEGFR2 signaling and that a decline in VEGFR2 signaling is required for arteriogenesis to fully take place. VEGF does not induce arterial fate in capillary ECs and, instead, counteracts FSS-driven capillary-to-arterial cell fate transition. Mechanistically, FSS-driven arterial program involves both Notch-dependent and Notch-independent events. Sox17 is the key mediator of the FSS-induced arterial specification and a target of VEGF-FSS competition. These findings suggest a new paradigm of VEGF-FSS crosstalk coordinating angiogenesis, arteriogenesis and capillary maintenance.

Arteriogenesis, defined as formation of new arteries in response to increasing input of blood flow, is determined by remodeling of the capillary bed and acquisition of arterial fate by capillary endothelial cells. Despite its physiological importance, how this process is regulated remains poorly understood.

In the past two decades, a wealth of studies suggested a widely accepted "VEGF-Notch-arterial fate" principle that highlights VEGF as the driver of arterial fate specification. This is based on data showing that VEGF induces Dll4[1-3], which in turn activates Notch[4-6], and that Notch is essential for arterial specification[7-9]. In the mouse retina, gain-of-function (GOF) constitutive Notch activation by overexpression of Notch intracellular domain (NICD) leads to increased and ectopic arterialization[10], while Notch loss-of-function (LOF) achieved by endothelial deletion of Dll4 or treatment with the gamma secretase inhibitor DAPT, results in a hypersprouting phenotype and defective arterial formation[4, 11-13]. Therefore, it is reasonable to infer that VEGF, as a Notch inducer, drives arterial specification. Moreover, a recent study proposed that a subset of endothelial cells (ECs) with high VEGF-Notch signaling at the vascular front are committed to arterial fate and that these "pre-arterial" ECs are later selectively acquire arterial fate[12, 14].

Besides VEGF, blood flow-derived fluid shear stress (FSS) has also been shown to induce Notch and arterial specification[15-17]. Notably, FSS-induced cell cycle G1/S arrest is reported as a pre-requisite for arterial fate acquisition[15]. This finding raises a question whether VEGF, as a mitogen that drives endothelial proliferation, really determines arterial specification. Although extremely high dose of VEGF or constitutive VEGFR2 signaling have been shown to induce cell cycle arrest[6, 18], these non-physiological stimuli do not exist in nature and thereby do not provide a definitive answer to address the role of VEGF in arterial specification. Moreover, if physiologically high VEGF signaling is the principal driver of arterial specification, one would expect to find arterialization at the vascular front in the developing retinal vasculature where VEGF levels are the highest and not towards the center of the retina where VEGF levels are declined. Further, it is unclear how the vascular front and the associated capillary bed avoid being ectopically arterialized, if VEGF is the driver of arterial specification, and how the capillary bed exposed to both VEGF and FSS maintain its capillary identity without undergoing premature arterialization. Finally, does nature really confer on VEGF a dual role in promoting both angiogenesis and arterial specification?

Interestingly, despite extensive studies of endothelial VEGFR2 signaling in angiogenesis, to our knowledge the role of VEGFR2 signaling in arterial fate specification has not been examined during the process of capillary bed remodeling. To address these critical issues, we set out to analyze postnatal arterial morphogenesis in mice with defective VEGFR2 signaling and model FSS-driven arterial specification in vitro. We find that arterial specification is driven by FSS and that capillary-to-artery endothelial cell fate transition requires a decline in VEGF signaling. Furthermore, VEGF signaling counteracts FSS-driven arterial fate acquisition by capillary endothelium. Mechanistically, FSS-induced arterial program involves Notch-dependent and primarily Notch-independent mechanisms. We show that SRY-box transcription factor 17 (Sox17) is the key to the FSS-arterial program and also a target of VEGF-FSS competition. Based on these findings, we propose a novel paradigm by which VEGF-FSS competition coordinates angiogenesis, arteriogenesis and capillary maintenance. This proposed model explains critical questions discussed above and reconciles the long-standing controversies in arterial specification.

Results

Arteriogenesis takes place in the capillary portion where VEGF signaling is declined.

Vascular morphogenesis in mouse postnatal retina begins at postnatal day 0(P0)-1 when nascent vessels sprout from the central vein[19, 20]. Our data show that a rudimentary capillary plexus emerges at P1-2 (Extended Data Fig.1). By P2-3 when a capillary bed has formed, arterial morphogenesis

identified by high-level expression of the arterial marker Sox17 (Sox17^{high}), appears in the central part of the capillary plexus (Extended Data Fig.1). At p3-4, while sprouting activity continues, leading the angiogenic front, arteriovenous patterning transforms the central portion of the capillary bed into a hierarchical vascular structure with capillaries, arteries and veins (Extended Data Fig.1). By p4-5, the whole vasculature has developed into a stereotypic vascular tree: the arteries and the veins alternatively aligned at the central area, the angiogenic sprouts at the periphery drive vascular expansion towards the avascular zone, and the capillary bed in bidirectional transition to the angiogenic sprouts towards the retinal periphery and to be remodeled as major vessels towards the retinal center, respectively (Extended Data Fig.1 and 2).

In this developing vasculature, the presence of endothelial phospho-ERK (pERK) signal and EdU-labeled proliferation activity mark the high level of VEGF signaling at the angiogenic front (Extended Data Fig. 2a-b). Of note, pERK and proliferation activity display a trend of decline in the capillary bed, especially in the capillary portion in transition to arteries with both almost completely disappearing in arterioles and arteries (Extended Data Fig.2a-b), consistent with previous reports. Systemic intravenous injection of VEGF activated pERK signaling in the whole vasculature, including the central portion of capillary bed and in arteries, where pERK signaling was absent in controls (Extended Data Fig.2b), confirming the decline of VEGF signaling in the endothelial cells (ECs) of this area. In summary, arterial morphogenesis takes place in the capillary portion where VEGF signaling has declined.

VEGFR2 signaling is not required for arterial specification; loss of VEGFR2 signaling results in increased arterialization.

To test the effect of endothelial VEGFR2 inactivation at various time windows, starting from the formation of a capillary bed before the onset of arteriogenesis, the first dosage of tamoxifen was given at P0, P1 or P2 to induce VEGFR2 deletion (*VEGFR2^{iECKO}*). As expected, induction at P0-2 (first dose at P0) led to the absence of vascular growth, leaving only a tiny vessel at the center of the retina at P5 (Extended Data Fig.3). Induction at P1-3 resulted in formation of vascular loops at P5, with striking reduction in radial outgrowth, branching activity and almost no sprouts (Fig.1a), consistent with previous reports[12, 13]. Notably, high level of Sox17 expression (Sox17^{high}) was detected in some morphologically arterial-like vessels spanning from the center to the vascular front in the *VEGFR2^{iECKO}* retina (Fig.1a). For quantitation purpose, arterial extension was defined as the percentage of arterial length within the complete vascular diameter at the specific location where the artery was measured. Based on this definition, arterial extension in the *VEGFR2^{iECKO}* retina was almost 100%, comparing with 56% in the control retina (Fig.1a). Moreover, smooth muscle coverage was detected in the central portion of the arteries in the control retina (Fig.1a). In the *VEGFR2^{iECKO}* retina, smooth muscle covered the full length of the arterial-like Sox17^{high} vessels and the venous-like vessels and at the vascular front (Fig.1a), suggesting the presence of both normal and ectopic arterialization. Likewise, induction of VEGFR2 deletion at P2-4 resulted in similar angiogenic and arteriogenic phenotypes (Fig.1b). Taken together, these data suggest that arterial specification is intact and, indeed, increased in the VEGFR2^{iECKO} retina.

To exclude the possibility of incomplete VEGFR2 deletion, we immunostained the retinas with anti-VEGFR2 antibody. In the control retina, VEGR2 signal was present in the blood vessels as well as the background of the neural bed (Fig.1b), consistent with previous report. Intriguingly, in the *VEGFR2^{iECKO}* retina, the VEGFR2+ neural bed negatively highlights the absence of VEGFR2 expression in blood vessels, making an appearance of “empty grooves” in a VEGFR2+ neural background (Fig.1b). This result confirms nearly complete deletion of endothelial VEGFR2. Notably, we detected VEGFR2^{null}/Sox17^{high} ECs in the artery-like vessels (Fig.1b), a direct evidence of arterial fate specification independent of VEGFR2.

Next, we examined arterial morphogenesis in postnatal retinas with endothelial deletion of PLCγ1 (*PLCγ1*^{iECKO}), the major effector of VEGF-A signaling[21, 22]. PLCγ is recruited to VEGFR2-Y1173 upon VEGF stimulation[21, 22]. As expected, the *PLCγ1*^{iECKO} retinas at P5 (following induction of deletion at P1-3), exhibited reduced sprouting activity and low capillary density, a typical angiogenic phenotype recapitulating the *VEGFR2*^{iECKO} retina, though to a somewhat lesser extent (Fig.1c). Similar to the arterial phenotype in *VEGFR2*^{iECKO}, in the *PLCγ1*^{iECKO} retinas Sox17^{high} ECs were present in arterial formations extending from retinal center to periphery, with increased number of side-branching arterioles (Fig.1c). Remarkably, a major artery was formed at the vascular front (Fig.1c), suggesting ectopic arterialization. Furthermore, smooth muscle coverage was detected in all major arteries as well as the peripheral area (Fig.1c). Overall, these results indicate intact arterial specification and increased arterialization in PLCγ1^{iECKO} retinas in line with the findings in *VEGFR2*^{iECKO} retinas.

Notch signaling, though not specific to artery, is an important arterial feature. In order to visualize Notch activity in the *VEGFR2*^{iECKO} and *PLCγ1*^{iECKO} mice, we crossed a Notch reporter line CBF:H2B-Venus[23] onto these strains of mice. In the control vasculature, Notch activity was clearly detected in arterial ECs but was undetectable in veins (Fig.2a). In the *VEGFR2*^{iECKO} and *PLCγ1*^{iECKO} vessels, Notch signal was detected in the Sox17^{high} ECs (Fig.2a). Staining of Dll4, a Notch ligand as well as a target, marked Notch activity in the angiogenic sprouts and arteries in control retinas (Fig.2b). In the *PLCγ1*^{iECKO} retinas, high level of Dll4 signal confirmed Notch activity in the arteries and some arterial-like vessels at the vascular front (ectopic arterialization) (Fig. 2b). These findings suggest that arterial Notch activity is independent of VEGFR2 signaling.

In conclusion, VEGFR2 signaling is not required for arterial morphogenesis during capillary remodeling; the loss of VEGFR2 signaling resulted in compromised angiogenesis and increased arterialization (summarized in Table 1). These findings strongly suggest that a genuine role of VEGF is to suppress arterialization, instead of promoting arterialization as it has long been thought in the field.

Fluid shear stress (FSS)-induced arterial specification is independent of VEGFR2 signaling.

Since VEGFR2 activity, and hence, VEGF, appear dispensable for arterial specification, we tested if FSS can serve that role. An important prerequisite for FSS as a driver of arteriogenesis is the presence of blood flow and, hence, lumenization of vessels in the VEGFR2^{iECKO} and PLCγ1^{iECKO} retinas. To address this question, we retro-orbitally injected Alexa488-conjugated isolectin B4 (IB4-488), which stains only the endothelium in patent vessels with blood circulation. After retinal dissection, we performed whole-mount counterstaining with Alexa594-conjugated IB4 (IB-594), which stains the whole vasculature, including the patent and the closed vessels. In the control retinas, while the majority of vessels was double-stained, the absence of IB4-488 negatively highlighted the un-lumenized sprouts at the vascular front and some regressed vessels around the arteries (Fig.3a), indicating a lack of blood flow in these vessels. Importantly, the VEGFR2^{iECKO} and the PLCγ1^{iECKO} vessels were well double-stained (Fig.3a), suggesting that there was effective blood flow through these vessels and that the ECs with defective VEGFR2 signaling were exposed to the hemodynamic force (FSS) as a potential driver for arterial specification.

We next tested FSS-driven arterial specification and Notch signaling in endothelial cells (HUVECs) with siRNA-silenced VEGFR2 or PLCγ1. HUVECs treated with either siVEGFR2 or siPLCγ1 were able to respond to arterial level of laminar FSS (12 dynes/cm^2) with induction of a panel of arterial genes, including Sox17, EFNB2, GJA4, GJA5 and Notch target Hey1 to the same extent as controls HIVECs treated with siCTRL (Fig.3b). Thes in vitro findings are consistent with the arterial phenotypes of VEGFR2^{iECKO} and PLCγ1^{iECKO} (Fig.1-2, Table1). We conclude that FSS-induced arterial specification and Notch activation is independent of VEGFR2 signaling.

VEGF counteracts FSS-induced capillary-to-artery endothelial cell fate transition.

To address how the capillary bed, which is exposed to both VEGF and FSS, avoids premature arterialization, we studied whether VEGF counteracts FSS-driven arterial specification to maintain capillary identity and prevent premature arterial fate transformation. To test this hypothesis, we used human microvascular blood endothelial cells (HMVBECs) to examine FSS-induction of arterial genes in the absence or presence of VEGF. HMVBECs are capillary ECs from juvenile dermal preparation without lymphatic ECs and thereby most representative of capillary features.

Our data showed that, under static (no flow) condition (ST), VEGF does not induce transcription of arterial genes, including Sox17, GJA4, GJA5, EFNB2, Nrp1, Sema3G and Jag1 (Fig.4a). By contrast, these genes were effectively induced by 16h of FSS (Fig.4a). Importantly, VEGF inhibited FSS-induced arterial program in a dose-dependent manner (Fig.4a-b). Blocking VEGF signaling by silencing PLCγ1 effectively rescued VEGF inhibition of the FSS-arterial program (Fig.4c-d).

To further understand gene expression changes regulated by the VEGF-FSS competition, we carried out RNAseq of HMVBECs under four different conditions: ST, ST+VEGF, FSS, FSS+VEGF (Fig.5). A PCA separation of the transcriptomic responses and differentially expressed arterial and capillary genes may suggest that ECs assume different cell states under these conditions (Fig.5a). To understand cell state transitions based on the acquired transcriptomics patterns, we applied elements of a systems biology approach termed cell State Transition Assessment and Regulation (cSTAR)[24-26] (Fig.5b). The first cSTAR element uses machine learning techniques, such as support vector machines (SVM) to exploit the high-dimensional omics space and construct separating surfaces between distinct EC states. Subsequently, the directions of EC state conversions are determined in the transcriptomic space. These directions are the shortest paths from one EC state to another state, which are specified by the State Transition Vectors (STVs), which are unit vectors defined as normal vectors to the hyperplanes that separate EC phenotypic states. After building the STVs, cSTAR calculates quantitative indicators of cell phenotypic states termed Dynamic Phenotype Descriptors (DPD). For EC cells in different states, the DPD scores describe phenotypic features associated with each STV[24, 25].

The STV_{FSS} indicates the shortest path from an EC ST state to a FSS state, and the DPD_{FSS} quantifies a normalized FSS-related score of the changes in the transcriptomics patterns for different EC states (Methods). The STV_{VEGF} determines the direction from a STAT state to a new EC state caused by VEGF stimulation at zero FSS, whereas the DPD_{VEGF} scores quantify the extent of the transcriptomics changes related to VEGF stimulation. The angle between two directions of the transcriptomics changes, STV_{FSS} and STV_{VEGF} is 84 degrees (Fig. 5b). The near orthogonality of these two STVs suggests mutually independent transcriptomic changes between the FSS and VEGF EC states, with any slight deviation from orthogonality indicating a minor overlap in the regulatory pathways induced by FSS or VEGF.

To comprehend the changes in the transcriptomic profile of the FSS EC state brought about by VEGF stimulation, we built the STV_{SSVA} to determine the direction of the EC FSS state change induced by a combined FSS and VEGF stimulation. The resulting STV_{SSVA} appears to be almost orthogonal to both STVs determined above (the angle between the two vectors, STV_{SSVA} and STV_{FSS} is 89 degrees, and the angle between the STV_{SSVA} and the STV_{VEGF} is 87 degrees **(**Fig 5b). Based on the STV_{SSVA}, we next calculated the DPD_{SSVA} that scores the changes in the phenotypic cell features following combined FSS and VEGF treatment. Fig. 5b and Extended Table 1 show that a combined VEGF and FSS treatment only slightly increases the DPD_{VEGF} score of the FSS state and does not change the DPD_{FSS} score. Overall, the results of this cSTAR analysis indicate that the FSS+VEGF is a new cell state distinct from STAT, FSS and VEGF states, and that the ST, VEGF, FSS, FSS+VEGF conditions result in four different, metastable EC states. Thus, treatments with VEGF alone, FSS alone or a combination of FSS and VEGF lead to new EC states and not a reversion of FSS state by VEGF to the baseline

state. This suggests that there are distinct programs activated by both VEGF and FSS with little overlap between the two.

As arterial specification is a result of capillary remodeling, we wonder whether the transitions between these cell states represent the capillary-to-artery cell fate transition. Notably, differential gene expression analysis clustered arterial and capillary gene profiles reciprocally regulated by VEGF and FSS (Fig.5c-d): FSS induced arterial genes and suppressed the capillary genes; by contrast, VEGF inhibited the FSS-induced arterial genes and rescued the FSS-suppressed capillary genes (Fig.5c-d). Western blot validation showed that FSS suppressed capillary genes Mfsd2a and VEGFR3, which was rescued by VEGF (Fig.5e). Moreover, immunostaining of capillary markers Mfsd2a, VEGFR3 and TFRC demonstrated a restricted expression pattern in the capillaries and the veins in contrast to low or undetectable expression in the arteries (Fig.5f).

Taken together, these data indicate that during arterial specification the transition from capillary to arterial fate is regulated by VEGF-FSS competition (Fig.5g). Importantly, FSS not only induces arterial fate but also suppresses capillary fate while VEGF maintains the capillary fate by counteracting FSS-induced capillary-to-artery cell fate transition (Fig.5g).

VEGF and FSS utilize different mechanisms to activate Notch.

As an important arterial feature, Notch activation has been thought to be the central determinant of arterial specification. Although both VEGF and FSS induce Notch, our data showed that only FSS induced arterial fate, while VEGF did not (Fig.4-5). We wondered whether their differences in kinetics of Notch activity, as induced by VEGF and FSS, that can explain this observation.

Our data show that VEGF and FSS used distinctly different mechanisms to activate Notch signaling in HMVBECs (Fig.6 and Extended Table 1). Upon VEGF stimulation, cleavage of Notch intracellular domain (NICD) was detected as early as 5 minutes (min), peaked at 40 min and then declined (Fig.6a). This dynamic of VEGF-induced NICD was temporally consistent with the protein levels of Dll4 (Fig.6a). Gamma-secretase inhibitor DAPT effectively suppressed NICD generation, but barely altered the curve of VEGF-induced Dll4 expression (Fig.6a), suggesting that Dll4 is upstream of NICD. Silencing Dll4 completely abolished VEGF-induced NICD activity (Fig.6b). These findings demonstrate that VEGF relies on Dll4 to activate Notch (Fig.6c), in agreement with previous reports[1, 3].

FSS-induced increase in NICD activity appeared within 20 minutes and continued to ramp up until after 1 hour and was higher in magnitude that VEGF induction of NICD (2.2-fold at 20min and 2.7-fold at 60min). At the same time, a slight increase of Dll4 expression was first detected at 40min and then slowly increased, lagging behind the increase in NICD level (Fig.6a). Unlike VEGF-induced Dll4 that was not affected by DAPT, FSS-induction of Dll4 was completely abolished when Notch activity was inhibited by DAPT (Fig.6a). Moreover, though siDll4 led to a much lower baseline of NICD, FSS still triggered NICD activity when Dll4 was depleted (Fig.6b). These results indicate that FSS does not rely on an increase of Dll4 to activate Notch and suggest that Dll4 is a Notch target gene activated by FSS-induced Notch signaling (Fig.6d). In summary, VEGF and FSS use distinctly different mechanism to activate Notch (summarized in detail in Extended Table 2). FSS-induced Notch activity is in higher magnitude and more persistent (Extended Table 2).

Since constitutive Notch activation is known to induce arterialization[10, 15], we wondered whether FSS induces a persistent pattern of Notch activity to drive arterial specification. Unexpectedly, in a 20-hour (20h) time course, FSS-induced Notch activity displayed a dynamic curve instead of being persistent (Fig.6e). FSS-induced NICD activity peaked at 1h and then declined at 3h until it reached 0.3-fold below the baseline at 6h. This was followed by a second wave of NICD activity ramping up from 9 to 20h (Fig.6e). Meanwhile, FSS induction of arterial genes (Sox17, EFNB2 and Sema3G) emerged at 6h when Notch activity reached the lowest level below baseline, and kept ramping up from

6 to 20h (Fig.6e). Of note, the FSS induction curves of the arterial genes tested here were not at all parallel to the dynamic of FSS-Notch activity, except for Dll4 (Fig.6e). Therefore, FSS does not rely on persistent Notch activity to induce arterial program.

Interestingly, VEGF did not alter the dynamic of the first wave of FSS-Notch activity from 0 to 6 hours (Fig.6e). Instead, it caused a lack of the second wave of Notch activity between 9-20 h, which is associated with reduced induction of the arterial genes (Fig.6e).

The FSS induction of arterial program is primarily Notch-independent.

Our observations summarized above (Fig.6) lead to two important questions: 1) When VEGF is added to FSS system, does the lack of a second wave FSS-Notch activity explain the reduced induction of FSS-arterial program? 2) Since the dynamic of FSS-Notch does not align with the induction curves of arterial genes, is it possible that FSS uses a Notch-independent mechanism to drive arterial specification? To answer these questions, we examined FSS-induced expression of arterial genes in a background of Notch inhibition induced by 5μM DAPT. HMVBECs were pretreated with DAPT for 3h to eliminate Notch activity before the initiation of FSS (Fig.7a). Most arterial genes tested remained effectively induced by FSS in the background of Notch inhibition (Fig.7a). Induction of Sox17, Sema3G, NRP1 and Jag1 under Notch inhibition were in comparable levels of induction under DMSO (Fig.7a); induction of EFNB2, Cx37 and Cx40 under Notch inhibition remained effective but displayed a substantial reduction (Fig.7a); induction of Dll4 was largely compromised by Notch inhibition (Fig.7a), consistent with the result in Fig.6a. These findings conclude that the FSS uses primarily a Notch-independent mechanism to activate the arterial program. Intriguingly, VEGF suppression of the FSS-arterial program remained effective under Notch inhibition (Fig.7a), suggesting that VEGF does not use Notch as a primary mechanism to compete with the FSS-arterial program.

These findings contradict the widely accepted understanding that FSS-arterial program is Notch-centered, and that Notch inhibition leads to defective arteriogenesis. However, underlying this seemly impeccable understanding, we notice two hidden issues that have long been neglected by the field. First, not all arterial ECs harbor high level of Notch activity (Fig.7b). We examined arterial Notch activity using the Notch reporter line CBF:H2B-Venus[23]. Our data show that 13.26% of the Sox17^{high} ECs did not colocalize with CBF-Venus signal (Fig.7b), indicating undetectable Notch activity in these arterial ECs. Second, due to the loss of negative feedback targeting VEGFR2[2, 27, 28], Notch inhibition in vivo results in uncontrolled VEGFR2 signaling, which simultaneously counteracts the FSS-arterial program according to our findings (Fig.4-5) and leads to unproductive vascularization with poor perfusion[29] (thereby low FSS) (Extended Fig.4). We hypothesize that, in the background of Notch inhibition, defective arteriogenesis is an indirect result secondary to these two primary phenotypes and that arterial specification can take place when VEGFR2 signaling is blocked. To this end, we injected 3 consecutive doses (P1-3) of DAPT to create a continuous Notch inhibition background before dissection at P4. At the same time, tamoxifen was added to the injection to induce endothelial deletion of PLCγ1 in order to block VEGFR2 signaling. As expected, the control retina with DAPT treatment exhibited a hypersprouting vasculature, in which no arterial morphogenesis were detected (Fig.7c). By contrast, in the PLCγ1^{iECKO} mice treated with DAPT, notable Sox17^{high} ECs highlighted the formation of arteries in substantial length, accompanied with significant reduction in vascular density (Fig.7c). This finding, in line with our in vitro data (Fig.7a), clearly demonstrates that, when VEGFR2 signaling is blocked, arterial morphogenesis occurs independent of Notch.

Sox17 is the key to mediate the FSS-arterial program and a target for VEGF-FSS competition.

Our finding that the FSS-arterial program is primarily Notch-independent suggests an unknown mechanism that FSS uses to drive arterial fate. We wondered whether arterial genes share any

common transcription regulator(s) that mediates the FSS-artery program targeted by VEGF signaling. Using bioinformatic tool TRANSFACT to interrogate potential common transcription factors for arterial, Notch and capillary genes, we found predicted Sox17 binding motifs in all arterial and Notch genes, including Sox17 itself, but not in the capillary genes (Extended Table2). Intriguingly, though most arterial genes share predicted binding motifs for Notch transcription regulator Rbpj, it is not found in the whole genomic sequences of Sox17 and Cx37. (Extended Table2). These findings suggest that Sox17 is a unique transcription factor for the arterial program.

Sox17 is indispensable for arterial specification in vivo[10] and can be induced by FSS (Fig.3-5). Nevertheless, it is unclear whether Sox17 is required for the FSS-arterial program and whether it is target for VEGF signaling to counteract the FSS-arterial program. Our data showed that CRISPR cas9-mediated deletion of Sox17 compromised the FSS-arterial program (Fig.8a). Also, lentivirus-delivered expression of Sox17 (Sox17-DDK-myc), when in a physiological level (8.26-fold) comparable to FSS-induced Sox17, activated the arterial program at static condition (Fig.8b). Remarkably, in the presence of VEGF, despite a much higher level (31-fold) of lentiviral Sox17 expression, the induction of arterial genes was either significantly reduced (Cx40, Cx37, Jag1) or insignificantly increased (EFNB2, Dll4) (Fig.8b). This finding indicates that Sox17-induced arterial program is effectively suppressed by VEGF, which bypasses FSS but completely recapitulates VEGF-FSS competition on the arterial program. Collectively, our data define Sox17 as the key to the FSS-arterial program as well as a pivotal target for the competing signaling from VEGF(Fig.8c).

Discussion

Vascular morphogenesis in the mouse postnatal retina involves several complex, well-coordinated processes (Fig 9A). Venous endothelial cells proliferate, migrate against blood flow and contributes to the formation of the capillary bed, sprouts at the front and the arteries[30, 31]. Similarly, capillary ECs contribute to sprouting and arterial ECs[32]. Tip cells at the vascular front undergo tip-stalk conversion, merge into capillary and tailed down to the arteries[31]. Finally, arterial endothelial cells remain where they are and do not contribute to other endothelial beds[32]. Taken together, the process of retinal vascular development starts with the vein at the retinal center sprouting to form a capillary bed, which then undergoes bidirectional transitions to the peripheral angiogenic front and remodels into a hierarchical arterial/venous circulation (Fig.9A). The entirety of this vascular morphogenesis, which involves angiogenesis, capillary formation and maintenance, and arteriogenesis, is guided by two major environmental cues: 1) a gradient of VEGF, produced by the avascular, hypoxic neural bed, and 2) FSS, the hemodynamic force exerted by the flow of blood through lumenized vessels (Fig.9B). VEGF-guided sprouting angiogenesis expands vascularization to meet the increasing demand of oxygen and nutrient supply during organogenesis, while FSS-driven arteriogenesis transforms part of the capillary bed into arteries to accommodate growing input of blood flow (Fig.9B). Subjected to both VEGF and FSS, the capillary bed needs to maintain capillary identity for oxygen and nutrient transport to underlying tissues, while the proximal arterial circulation is needed to deliver adequate volumes of blood flow (Fig.9B).

Based on our data, we propose a novel paradigm: competing signals from VEGF and FSS control the balance of angiogenesis, capillary maintenance and arteriogenesis (Fig.9B). In the case of the retina, its postnatal growth results in continuous expansion of the avascular zone, where hypoxia induces high level of VEGF to trigger angiogenic sprouting. As expanding vascularization brings oxygen to resolve hypoxia, it ceases VEGF production from the newly vascularized microenvironment as well as the signaling activities it induces in ECs. This creates a permissive condition for FSS to drive capillary-to-artery cell fate transition and ultimately the specification of arterial fate. Besides its role in angiogenic sprouting, VEGF also maintains the capillary bed by counteracting the FSS-arterial program, which prevents the capillary bed from premature arterialization.

Our data show that the loss of VEGFR2 signaling (*VEGF LOF*) causes not only defective sprouting, but also increased and ectopic arterialization (Fig.1). Without VEGF signaling to protect the capillary fate, FSS-driven excessive arterialization compromises the size of the capillary bed adversely affecting tissue oxygenation. On the other hand, uncontrolled VEGF signaling (*VEGF GOF*), on the background of Notch inhibition (due to the loss of negative feedback to VEGFR2 signaling), results in formation of a high-density capillary bed that, nevertheless, lacks effective tissue perfusion. Arteriogenesis is defective in this animal model, but can be rescued by blocking VEGFR2 signaling (Fig.7). This finding suggests that high VEGF signaling inhibits arterial formation and also indicates that arteries can form independent of Notch signaling (Fig.7).

Our data show that the FSS-induced arterial program does not require and is independent of VEGF, as it remains intact in animal and in vitro models with defective VEGFR2 signaling (Fig.1-3). Our data also clearly indicate that VEGF treatment does not induce arterial fate in capillary ECs and that FSS-induced arterial specification requires a permissive condition without active VEGFR2 signaling (Fig.4-5). These findings explain why physiological arterial formation occurs away from the vascular front, where arterialization normally does not occur due its inhibition by high levels of VEGF. Furthermore, arteriogenesis, as a result of capillary remodeling, involves not only a differentiation process to acquire arterial fate but also a process of cell migration against blood flow to form major arterial vessels. While our proposed model of VEGF-FSS competition addresses the mechanism underlying arterial differentiation, it is in line with a recent report showing that VEGF-FSS competition also modulates EC polarity and migration during capillary remodeling[33].

Notch signaling is an essential arterial feature. Based on observed arterial phenotypes in Notch LOF and GOF animal models, Notch has been thought to be the central determinant of arterial specification. Our data show that VEGF and FSS use distinctly different mechanisms to activate Notch (Fig.6). Although VEGF induces Dll4 expression, it does not lead to the induction of other arterial genes, which is different from the experiment of immobilized Dll4[15] known to induce arterialization. As to FSS-induced Notch, although FSS activates a higher magnitude of Notch signaling than VEGF, it demonstrates a dynamic with 2 waves of activities unparalleled with the induction curves of arterial genes (Fig.6). Therefore, unlike the artificial experiment using constitutive expression of NICD[10] known to induce arterialization, FSS does not rely on a persistent pattern of Notch activation to induce the arterial program.

Intriguingly, when VEGF and FSS, two well-known Notch inducers, are added together, there is no additive effects on the level of Notch signaling. On the contrary, it results in inhibition of the second wave of FSS-induced Notch activity (9-20h, Fig.6e), which at least accounts for reduced induction of the arterial genes partially (GJA4, GJA5, EFNB2) or completely (Dll4) dependent on Notch. Moreover, our data show that induction of some definitive arterial genes (Sox17, Sema3G, Nrp1 and Jag1) is almost completely independent of Notch signaling. In line with this in vitro finding, arteriogenesis in vivo occurs in the background of Notch inhibition when VEGF signaling is blocked. Taken together, FSS relies on primarily Notch-independent and additionally Notch-dependent mechanisms to induce arterial specification. In other words, Notch signaling partially contribute to arteriogenesis; as an essential arterial feature, Notch signaling is a consequence rather than a causative determinant of the FSS-arterial program.

Instead of Notch, Sox17 appears to be the central driver of the FSS-arterial program (Fig.8). SoxF family of transcription factors, Sox7, Sox17 and Sox18, are expressed by all ECs[34]. Among them, only Sox17 exhibits high-level expression in the arteries and has been reported to be indispensable for arterial specification[10, 34]. FSS induces Sox17, while VEGF does not[10] (Fig.4-5). We show that Sox17 is indispensable for the FSS-arterial program (Fig.8). Moreover, artificial expression of Sox17 bypasses FSS to activate the arterial program, which is inhibited by VEGF, a recapitulation of VEGF-FSS

competition on arterial specification (Fig.8). These findings define Sox17 as the central determinant of the FSS-arterial program and a target for competing signaling from VEGFR2.

Methods

Animal models

VEGFR2$^{flox/flox}$ mice (a gift kindly provided by Lena Claesson-Welsh, Uppsala University), *PLCγ1$^{flox/flox}$* mice (a gift kindly provided by Renren Wen, Wisconsin Blood Institute) were crossed with *Cdh5CreER^{T2}* mice (a gift kindly provided by Ralf Adams). *CBF:H2B-Venus* mice, purchased from Jackson Laboratory, were crossed with *VEGFR2$^{flox/flox}$; Cdh5CreER^{T2} mice or PLCγ1$^{flox/flox}$; Cdh5CreER^{T2} mice. VEGFR2$^{flox/flox}$; Cdh5CreER^{T2}* mice were in *C57Bl/6J* background*. PLCγ1$^{flox/flox}$; Cdh5CreER^{T2} mice were backcrossed to C57Bl/6J* background for 10 generations*.* Gene deletion was induced by three consecutive dosages of 100ug Tamoxifen via daily peritoneal injection. Tamoxifen powder (Sigma, T5648) was suspended in corn oil (Sigma, C8267) and then dissolved by agitation at 37°C for 2 hours (h). All mouse experimental procedures complied to the protocols approved by the Yale University Institutional Animal Care and Use Committee (IACUC). Genotyping primers are listed in Extended Table 4.

Retinal dissection

Mouse neonates were euthanized at postnatal day 5 (P5) or P6. Eyes were enucleated and immediately fixed with 4% paraformaldehyde (PFA) for 8 minutes (min) at room temperature (RT). Then the eyes were transferred to PBS to terminate pre-dissection fixation. Dissected retinas were fixed with 4% paraformaldehyde for 30 min at RT with gentle rocking, followed by 2 washes in PBS at RT, 5 min each. Retinas were subjected to immunostaining procedure or stored in methanol at -20°C. Retinas stored in methanol were warmed up at room temperature and rehydrated with PBS before immunostaining.

Immunostaining and confocal imaging

P5-6 retinas were incubated in wash buffer (PBS with 0.1%Triton X100) with gentle rocking for 15 min and then in blocking buffer (wash buffer with 5% normal donkey serum (Jackson ImmunoResearch, 017-000-121)) for 1-2 hrs. Blocked retinas were incubated with primary antibodies diluted in blocking buffer overnight at 4°C with gentle rocking. On the next day, the retinas were washed in wash buffer for 3 times, 15 min each. Secondary antibodies were mixed with isolectin B4 in blocking buffer, in which the retinas were incubated at RT for 1.5 h with gentle rocking in dark. The staining procedure was finished after 3 washes in wash buffer, 15 min each. The retinas were transferred to PBS without detergent before flat mount. Antibodies and experimental conditions were listed in Extended Table 5. Image acquisition was conducted with Leica TCS SP8 Confocal Laser Scanning Microscope. Leica LAS-X, Image J (NIH) and IMARIS (Bitplane, USA) were used for image analysis.

EdU labeling

50ug EdU (Sigma #900684) solution were peritoneally injected into mouse neonates at P5 4h before retinal dissection. Erg antibody (Abcam, # ab214341) was stained to visualize endothelial nuclei, followed by detection of EdU incorporation using EdU Cell Proliferation Kit (Invitrogen, #C10340).

Immunostaining of phospho-ERK1/2

Mouse neonates at P5 were placed on a warm pad at 37°C for 30min. The eyes were enucleated and immediately fixed in 4% PFA for 8 min, RT. Using ice-cold PFA will decrease fixation efficacy and

must be avoided at this step. The retinas were transferred to and dissected in ice-cold PBS. Post-dissection fixation in 4% PFA was done at 4°C with gentle rocking for 2 h. The fixed retinas were washed once with PBS for 5min, RT, and stored in ice-cold methanol at -20°C for 1 h. After warming up at RT for 15min, the retinas were rehydrated in PBS for 5min, followed by incubation in PBST (PBS with 0.25%Triton X100) for 30min and then blocking in PBST with 10% normal donkey serum (blocking buffer) for 1hr, RT. Phospho-p44/42 MAPK (Erk1/2) (Thr202/Tyr204) antibody (Cell signaling Technology, #9101) were diluted in blocking buffer. From this step, the staining procedure followed the regular protocol described above.

Vascular patency analysis

Mouse neonates at P5 or P6 were placed on a warm pad at 37°C for subsequent procedure of vascular perfusion. IB4-Alexa488 was diluted in PBS and retro-orbitally injected to visualize patent (lumenized) vessels. Calculation of IB4 dilution (1:50) was based on estimated blood volume 5.5ml/100g body weight (The Jackson Laboratory). 1:50= (IB4 volume) : (blood volume + injection volume). Injected pups were placed on warm pad for 20min, followed by retinal dissection procedure. Dissected retinas were counter-stained with IB4-Alexa 647 to visualize all vessels, lumenized and unlumenized.

Endothelial cell culture and flow (shear stress) systems

Human microvascular blood endothelial cells (HMVBECs) (HDBECs, Promocell, #C-12211) were maintained in EGM2-MV full growth medium (Lonza). Permissive arterial differentiation medium (PADM), made of EBM2 basal medium with 5% FBS, was used for flow-induced arterial differentiation. Approximately 6 h prior to start of flow, EGM2-MV medium was removed, followed by a wash and a refill with PADM. Human Umbilical Vein Endothelial Cells (HUVECs) (from Yale VBT) were maintained in M199 medium containing 20%FBS and endothelial cell growth supplements (aliquots of Corning product were purchased from Yale VBT). For HUVECs, the maintenance medium was used for flow-induced arterial differentiation.

HMVBECs or HUVECs were seeded in IBIDI µ-slides (0.4 Luer ibiTreat) (IBIDI, #80176), with an initial seed density of 0.12-0.15 x 10^6 cells per slide, and were maintained for 48 h in the slide channel before flow experiment.

Flow system was built with a mini peristaltic pump (Cole Parmer MasterFlex Peristaltic pump C/L drive P/N: 77122-22), an assembly of tubing systems with a pulse dampener and a medium reservoir. The tubing system was assembled with a coiled inlet tubing (60cm) and a coiled outlet tubing (160cm), a total length of 220cm to further weaken pulsation. The end of the outlet tubing was fit into the pump head to passively draw the flow out of the IBIDI channel instead of pumping in. A flow rate of 12ml/min, which creates 12 dynes/cm^2 shear stress according to the IBIDI manual, was accurately measured in each flow system prior to the start of each flow experiment. The flow systems were placed in cell culture incubator for 30min for equilibrium of temperature and CO_2 before connecting IBIDI µSlides.

Small interfering RNA (siRNA) experiments

FuGene SI transfection reagent (VWR, # MSPP-SI-1000) was used for siRNA transfection. HUVECs or HMVBECs were seeded in maintenance medium to reach a density of 80-90% on the day of transfection. siRNA/FuGene/OptiMEM mix was added to EGM2-MV full growth medium for 6h, followed by a wash with PBS and replacement with fresh EGM2-MV full medium. On the next day, the siRNA-treated cells were trypsinized and seeded in IBIDI µSlides with maintenance medium. Flow experiments started at 48h (siVEGFR2 and siDll4) or 72h (siPLCγ1) after siRNA transfection. siRNA information is listed in extended table 6.

RNA isolation and RT-qPCR

Qiagen RNeasy plus Mini kit (#74134) was used for total RNA isolation, followed by reverse transcription to synthesize cDNA using iScript cDNA Synthesis Kit (Bio-Rad, #170–8891). SYBR Green Supermix (Bio-Rad, #1798880) was used for qPCR. Cycle threshold (Ct) values of gene expression were subtracted from average housekeeping gene GAPDH, and relative quantification of experimental groups versus control was calculated. QPCR primers are listed in Extended Table 7.

RNA sequencing and bioinformatic analysis

Total RNA samples were sent to Yale Center for Genomic Analysis (YCGA) for quality analysis, library preparation and sequencing. Partek Flow was used for bioinformatic analysis. Briefly, adapters in RNAseq reads were trimmed, and the trimmed reads were aligned to aligner algorithm STAR. Normalized gene counts were analyzed using DESeq2 to determine differential gene expression.

Computational methods and cSTAR analysis. To analyze EC responses to FSS, VEGF and a combined FSS plus VEGF, the control condition is selected as no treatment, static condition (ST) and the log fold-changes of the differentially expressed genes with respect to ST were calculated. The SVM algorithm with a linear kernel from the scikit-learn python library was applied to build a maximum margin hyperplane that distinguishes four different EC states. The STVs are calculated as unit vectors, which are normal vectors to the three hyperplanes separating EC states. After building the STVs, cSTAR calculates quantitative indicators of cell phenotypic states termed DPDs. The DPD scores describe the changes in the cell phenotypic features that would occur when the data point crosses on the separating hyperplanes. The absolute value of the DPD score is determined by the Euclidean distances from the data point to the separating hyperplane, while the sign of the DPD score indicates if the direction of the data point movement to cross the hyperplane is parallel or antiparallel to the corresponding STV[25]. The DPD scores were normalized so that the DPD values in the training set (FSS, VEGF, and FSS-VEGF states) were -1, 0 or 1. All codes of building STVs and calculating the normalized DPD scores will be provided in a journal publication.

Western blots

The following recipe was used to prepare lysis buffer for detecting Connexins and other proteins. A tablet of protease inhibitor cocktail (Roche) and a tablet of PhosSTOP were dissolved in 4.75ml water. Then the following reagents were sequentially added and then mixed: 1.25ml 1M Tris, 2ml 20%SDS, 2ml Glycerol, 1ml beta-mercaptoethanol and a tip amount of blumophenol blue. To harvest protein lysate from IBIDI µSlide, medium was removed from the channel and replaced with 150ul lysis buffer. To enhance protein lysing, the IBIDI µSlide with lysis buffer was subject to a freezing-thawing cycle, then repeatedly tilted several times before retrieving protein lysate. Protein lysate was collected in centrifuge tube and sonicated for 1 min at 15% power, followed by heating at 75°C for 30 min to denature protein. Antibodies used for western blot were listed in Extended Table 8.

Lentiviral Sox17 expression and induction of arterial differentiation

Lentiviral construct pBob-hSox17-DDK-Myc was created in the Simons lab and can be shared upon reasonable request. To induce arterial differentiation, HUVECs were seeded in the M199-based maintenance medium described above to reach a density of 90% on the day of transduction. On day1, the medium was replaced with EGM2-MV full media for lentiviral transduction for 24 h, followed by a wash with PBS and replacement with fresh EGM2-MV full media on day2. On day3 when cell density reached 100% as a monolayer (critical for consistent arterial differentiation), EGM2-MV full media was

removed, washed, and switch back to the M199-based maintenance medium for arterial differentiation. Samples were collected on day4 (48h after the end of transduction) for analysis.

CRISPR-cas9-mediated gene deletion

Oligos of designed gRNA sequences were cloned into lentiCRISPRv2 (Addgene #52961) following previously published protocol[35]. The following gRNA sequences were used, including a non-targeting gRNA (GTATTACTGATATTGGTGGG) and a pair of gRNAs targeting human Sox17 (ACGGGTAGCCGTCGAGCGG and GGCACCTACAGCTACGCGC)[36]. HUVECs transduced with lentiviral-delivered sgRNAs were selected with 0.8ug/ml puromycin for 48hrs and maintained in EGM2-MV medium for a total of 7 days to allow gene recombination. This was followed by a second cycle of selection with puromycin for 48hrs and recovery for 3 days before seeding the cells to the IBIDI µ slides for flow experiments. Cas9 expression and deletion of Sox17 were assayed by western blot.

Statistics

Data was plotted using GraphPad Prism8.0.0 or Microsoft Excel version 2310. Student's t test was used for comparison of two groups, with the assumption of normal distribution and equal variance between groups. All experiments were repeated at least 3 times to acquire samples with biologically difference. A p value less than 0.05 was considered as statistically significant.

Acknowledgements

We thank Prof. Lena Claesson-Welsh for providing the *VEGFR2*$^{flox/flox}$ mice, Prof. Ralf Adams for providing the *Cdh5CreER*^{T2} mice and Prof. Renren Wen for providing the *PLCγ1*$^{flox/flox}$ mice. We thank Drs. Prajwal Boddu, Emma Ristori and Federico Corti for important technical advice on gene cloning. We thank Rolando Milian, Yale Medical Library, for bioinformatic training and assistance of RNAseq data analysis. We thank Guilherme Dantas for technical assistance in immunostaining and confocal imaging and Tuo Guo for assistance in vascular quantification. This work was supported by NIH grants R01HL169520-01, P01HL107205-06A1, NIH/NCI grant R01CA244660 and EU grant no. 101136926 MULTIR (BNK), Science Foundation Ireland 22/PATH-S/10875 (OSR) and Open Philanthropy.

Figure 1: VEGFR2 signaling is not required for arterial fate specification during capillary remodeling.

a. Control and *VEGFR2*^{iECKO} mouse postnatal retinas dissected at p5 (tamoxifen-induced gene deletion at p1-3). Retinas were immunostained with Isolectin B4 (IB4) and antibodies targeting smooth muscle actin (SMA) and Sox17. Pink arrow heads indicate ectopic SMA signal at the vascular front and the vein. Arterial extension is the percentage of the length of arteries normalized by the diameter of vascular outgrowth. b. Control and *VEGFR2*^{iECKO} mouse postnatal retinas dissected at p6 (tamoxifen-induced gene deletion at p1-3). Retinas were immunostained with IB4 and VEGFR2 to visualize endothelial deletion of VEGFR2. White arrow heads indicate Sox17^{high}/VEGFR2^{+} ECs in the control mice. Blue arrow heads indicate Sox17^{high}/VEGFR2^{null} ECs. c. Control and *PLCγ1*^{iECKO} mouse postnatal retinas dissected at p5 (tamoxifen induction of gene deletion at p1-3). Retinas were immunostained with IB4 and antibodies targeting Sox17 and SMA. Abbreviations: A: artery; V: vein. Scale bars: 100µm.

Figure 2: Arterial Notch activation is independent of VEGFR2 signaling.

a. Control, *VEGFR2*^{iECKO} and *PLCγ1*^{iECKO} mice were crossed with Notch reporter line CBF:H2B-Venus to visualize Notch activity. Mouse postnatal retinas dissected at p5 (tamoxifen-induced gene deletion at p1-3) were immunostained with IB4 and Sox17 antibody. Nuclear CBF signal was natural fluorescence from Venus. Two tailed, unpaired Student t-test was used for statistics. $p<0.05$ was determined as statistically significant. b. Mouse postnatal retinas from Control and *PLCγ1*^{iECKO} mice were dissected at p5 (tamoxifen induction of gene deletion at p1-3) and immunostained with IB4 and Dll4 antibody. Abbreviations: A: artery; V: vein. Scale bars: 100µm.

Figure 3: Fluid shear stress-induced arterial specification is independent of VEGFR2 signaling.

a. Mouse postnatal retinas were dissected at p5 (tamoxifen-induced gene deletion at p1-3). Before dissection, IB4 (green) was retro-orbitally injected to perfuse the retina vasculatures of Control, *VEGFR2*^{iECKO} and *PLCγ1*^{iECKO} mice. Dissected retinas were stained with IB4 (red) to visualize all perfused and non-perfused blood vessels. Perfused vessels are double-stained (IB4-green/red), while non-perfused vessels were single-stained (IB4-red only, indicated by white arrow heads). Abbreviations: A: artery; V: vein. Scale bars: 100µm. b. HUVECs with siRNA treatments were subjected to static (ST) or FSS (12dyn/cm^2) for 16 hours to induce arterial differentiation. Gene expression was examined by quantitative RT-PCR followed by quantification relative to ST-siCTRL. Student t-test was used for statistics. $p<0.05$ was determined as statistically significant. ns: not significant.

Figure 4. VEGF counteracts FSS-induced arterial specification.

a. HMVBECs were used to test the induction of arterial and Notch genes under the conditions of static (ST), ST with VEGF (20ng/ml), FSS (12dyn/cm^2) and FSS with VEGF. Gene expression was examined by quantitative RT-PCR followed by quantification relative to ST. b. FSS-induced expression of GJA4, GJA5 and Hey1 in HMVBECs with a gradient of VEGF. Gene expression was examined by quantitative RT-PCR followed by quantification relative to ST. FSS experiments were conducted using Vitroflo system. All conditions under FSS were in the same Vitroflo plate. c. HUVECs treated with siRNA were used to test FSS-induced expression of arterial genes and the effect of VEGF. d. A working model demonstrating VEGF signals through VEGFR2-PLCγ1 to counteract FSS-induced arterial specification. Student t-test was used for statistics. $p<0.05$ was determined as statistically significant. ns: not significant.

Figure 5. VEGF-FSS competition regulates capillary-to-artery cell fate transition.

a. Principal component analysis (PCA) of RNAseq data. b. cSTAR analysis of RNAseq data. DPD scores of EC states shown in 3D space of the STVFSS, STVVEGF, and STVSSVA. Four EC states correspond to different FSS and VEGF treatments. A change in the EC phenotype is quantified by the DPD score along the corresponding STV. c. Differential gene expression clustered the arterial and capillary genes. d. Volcano plots demonstrating differential expression of the arterial and capillary genes under conditions of FSS versus ST and FSS+VEGF versus FSS, respectively. e. Expression of the arterial and capillary genes examined by wester blots. f. Immunostaining of capillary genes Mfsd2a, VEGFR3 and TFRC in P5 mouse retina. g. A working model: competing signals from VEGF and FSS regulate cell fate transition between capillary and arterial fates.

Figure 6. VEGF and shear stress use distinctly different mechanisms to activate Notch.
a. HMVBECs were subjected to VEGF (20ng/ml) or FSS (12 dyn/cm^2) to test the activation of Notch signaling in a time course, with DMSO or γ-secretase inhibitor DAPT treatments. b. HMVBECs treated with siCTRL or siDll4 were subjected to VEGF and FSS to test the activation of Notch signaling. c-d. Working models demonstrating the mechanisms by which VEGF and FSS use to activate Notch signaling. VEGF activates the expression of Dll4, which consequently serves as a ligand to activate Notch signaling in a neighboring cell. By contrast, FSS does not rely on increasing Dll4 expression to activate Notch. Increase of Dll4 expression is a result rather than a cause of FSS-induced Notch activation. e. FSS-induced Notch signaling and expression of arterial genes. HMVBECs were subjected to FSS in a time course in the absence or presence of VEGF.

Figure 7. The FSS-arterial program is primarily Notch-independent.
a. Pretreated with DMSO or 5uM DAPT for 3h, HMVBECs were subjected to FSS to induce arterial differentiation for 16h. Samples were analyzed by western blot. b. Representative retinal artery and branching arterioles at p5 from the Notch reporter mouse line CBF:H2B-Venus. Arterial ECs were labeled by immunostaining of Sox17 and colocalized with endogenous Venus signal in the nuclei. Arrow heads indicate Sox17^{high}/CBF- arterial ECs. Scale bars: 25 µm. c. In the background of DAPT-induced Notch inhibition (P1-3), arterial morphogenesis in P4 retina from control and *PLCg1*^{iECKO} mice. White arrow heads indicate arterial morphogenesis marked by Sox17^{high} ECs; yellow arrow heads indicate smooth muscle coverage. Abbreviations: A: artery; V: vein. Scale bars: 100 µm.

Figure 8. Sox17 is the key to mediate the FSS-arterial program and a target for VEGF-FSS competition.
a. HUVECs with CRISPR-Cas9-directed sgNT or sgSox17 were subject to FSS to induce arterial differentiation. ST: Static. FSS: fluid shear stress. sgNT: non-targeting guide RNA. SgSox17: guide RNA targeting Sox17. b. Western blot of lentivirus-delivered expression of Sox17 dual-tagged with Flag and Myc (Sox17-DDK-Myc) in HUVECs. c. Working model demonstrating the interaction between VEGFR2 signaling and Sox17-mediated FSS-arterial program.

Figure 9. Working model: VEGF and FSS counteract to regulate angiogenesis, capillary maintanance and arteriogenesis.
a. Trajectory of vascular morphogenesis. The whole vasculature originates from the vein, which gives rise to the capillary bed. The capillary bed expands by sprouting angiogenesis towards the peripheral avascular zone, and, at the same time, undergoes a remodeling process to form arteries. b. Gradients of VEGF and FSS counteract to control angiogenesis and arteriogenesis from the capillary bed. The condition with high level of VEGF and low FSS favors angiogenesis and inhibits arteriogenesis, while

arteriogenesis requires a decline of VEGF signaling as a permissive prerequisite and high arterial level of FSS to drive arterial specification.

Table 1. Vascular phenotypes result from defective VEGFR2 signaling.

Extended data figure1. Capillary bed formation and remodeling in mouse postnatal retina.
Mouse retinas were dissected at P1-4, followed by immunostaining of Sox17 and IB4 to label arteries and the whole vasculature. The arrow in P2 indicates emergence of arterial morphogenesis as labeled by high level of Sox17 expression. Abbreviations: A: artery; V: vein. Scale bars: 100µm.

Extended data figure 2. Arteriogenesis occurs in the capillary portion where VEGF signaling is declined.
a. P5 retina was immunostained with EdU, Erg and IB4. b. Immunostaining of pERK and IB4 on P5 retina. i.v.: intravenous (retro-orbital) injection. Scale bars: 100µm.

Extended data figure 3. Deletion of endothelial VEGFR2 at P0 results in no vascular morphogenesis.
Immunostaining of control and VEGFR2^{iECKO} retinas at P5. Tamoxifen was injected at P0-2.

Extended figure 4. Working model: in the background of Notch inhibition, defective arteriogenesis is an indirect result secondary to uncontrolled VEGFR2 signaling.
Notch signaling is an essential negative feedback mechanism targeting VEGFR2 signaling. The direct consequence of Notch loss-of-function (LOF) is uncontrolled, high level of VEGFR2 signaling, which 1) leads to uncontrolled angiogenesis generating dense but poorly lumenized capillaries with minimal FSS and 2) counteracts the FSS-arterial program.

Extended Table 1. A matrix of the DPD scores.

Extended table2. VEGF and FSS use distinctly different mechanisms to activate Notch.

Extended table3. Predicted transcription factor binding motifs of Sox17 and RBPJ in arterial and capillary genes (TRANSFACT).

Extended Table 4. Genotyping primers

Extended Table 5. Antibodies for immunostaining.

Extended Table 6. siRNA information.

Extended Table 7. QPCR primers

Extended Table 8. Antibodies for western blot.

Reference

1. Wythe JD, Dang LT, Devine WP, Boudreau E, Artap ST, He D, Schachterle W, Stainier DY, Oettgen P, Black BL, Bruneau BG, Fish JE. Ets factors regulate vegf-dependent arterial specification. *Dev Cell*. 2013;26:45-58
2. Lobov IB, Renard RA, Papadopoulos N, Gale NW, Thurston G, Yancopoulos GD, Wiegand SJ. Delta-like ligand 4 (dll4) is induced by vegf as a negative regulator of angiogenic sprouting. *Proc Natl Acad Sci U S A*. 2007;104:3219-3224
3. Liu ZJ, Shirakawa T, Li Y, Soma A, Oka M, Dotto GP, Fairman RM, Velazquez OC, Herlyn M. Regulation of notch1 and dll4 by vascular endothelial growth factor in arterial endothelial cells: Implications for modulating arteriogenesis and angiogenesis. *Mol Cell Biol*. 2003;23:14-25
4. Hellstrom M, Phng LK, Hofmann JJ, Wallgard E, Coultas L, Lindblom P, Alva J, Nilsson AK, Karlsson L, Gaiano N, Yoon K, Rossant J, Iruela-Arispe ML, Kalen M, Gerhardt H, Betsholtz C. Dll4 signalling through notch1 regulates formation of tip cells during angiogenesis. *Nature*. 2007;445:776-780
5. Kopan R, Ilagan MX. The canonical notch signaling pathway: Unfolding the activation mechanism. *Cell*. 2009;137:216-233
6. Ubezio B, Blanco RA, Geudens I, Stanchi F, Mathivet T, Jones ML, Ragab A, Bentley K, Gerhardt H. Synchronization of endothelial dll4-notch dynamics switch blood vessels from branching to expansion. *Elife*. 2016;5
7. Hasan SS, Tsaryk R, Lange M, Wisniewski L, Moore JC, Lawson ND, Wojciechowska K, Schnittler H, Siekmann AF. Endothelial notch signalling limits angiogenesis via control of artery formation. *Nat Cell Biol*. 2017;19:928-940
8. Lawson ND, Scheer N, Pham VN, Kim CH, Chitnis AB, Campos-Ortega JA, Weinstein BM. Notch signaling is required for arterial-venous differentiation during embryonic vascular development. *Development*. 2001;128:3675-3683
9. Roca C, Adams RH. Regulation of vascular morphogenesis by notch signaling. *Genes Dev*. 2007;21:2511-2524
10. Corada M, Orsenigo F, Morini MF, Pitulescu ME, Bhat G, Nyqvist D, Breviario F, Conti V, Briot A, Iruela-Arispe ML, Adams RH, Dejana E. Sox17 is indispensable for acquisition and maintenance of arterial identity. *Nat Commun*. 2013;4:2609
11. Benedito R, Trindade A, Hirashima M, Henrique D, da Costa LL, Rossant J, Gill PS, Duarte A. Loss of notch signalling induced by dll4 causes arterial calibre reduction by increasing endothelial cell response to angiogenic stimuli. *BMC Dev Biol*. 2008;8:117
12. Pitulescu ME, Schmidt I, Giaimo BD, Antoine T, Berkenfeld F, Ferrante F, Park H, Ehling M, Biljes D, Rocha SF, Langen UH, Stehling M, Nagasawa T, Ferrara N, Borggrefe T, Adams RH. Dll4 and notch signalling couples sprouting angiogenesis and artery formation. *Nat Cell Biol*. 2017;19:915-927
13. Zarkada G, Heinolainen K, Makinen T, Kubota Y, Alitalo K. Vegfr3 does not sustain retinal angiogenesis without vegfr2. *Proc Natl Acad Sci U S A*. 2015;112:761-766
14. Red-Horse K, Siekmann AF. Veins and arteries build hierarchical branching patterns differently: Bottom-up versus top-down. *Bioessays*. 2019;41:e1800198
15. Fang JS, Coon BG, Gillis N, Chen Z, Qiu J, Chittenden TW, Burt JM, Schwartz MA, Hirschi KK. Shear-induced notch-cx37-p27 axis arrests endothelial cell cycle to enable arterial specification. *Nat Commun*. 2017;8:2149
16. Masumura T, Yamamoto K, Shimizu N, Obi S, Ando J. Shear stress increases expression of the arterial endothelial marker ephrinb2 in murine es cells via the vegf-notch signaling pathways. *Arterioscler Thromb Vasc Biol*. 2009;29:2125-2131
17. Kim D, Grath A, Lu YW, Chung K, Winkelman M, Schwarz JJ, Dai G. Sox17 mediates adult arterial endothelial cell adaptation to hemodynamics. *Biomaterials*. 2023;293:121946
18. Pontes-Quero S, Fernandez-Chacon M, Luo W, Lunella FF, Casquero-Garcia V, Garcia-Gonzalez I, Hermoso A, Rocha SF, Bansal M, Benedito R. High mitogenic stimulation arrests angiogenesis. *Nat Commun*. 2019;10:2016

19. Gerhardt H, Golding M, Fruttiger M, Ruhrberg C, Lundkvist A, Abramsson A, Jeltsch M, Mitchell C, Alitalo K, Shima D, Betsholtz C. Vegf guides angiogenic sprouting utilizing endothelial tip cell filopodia. *J Cell Biol*. 2003;161:1163-1177
20. Stahl A, Connor KM, Sapieha P, Chen J, Dennison RJ, Krah NM, Seaward MR, Willett KL, Aderman CM, Guerin KI, Hua J, Lofqvist C, Hellstrom A, Smith LE. The mouse retina as an angiogenesis model. *Invest Ophthalmol Vis Sci*. 2010;51:2813-2826
21. Takahashi T, Yamaguchi S, Chida K, Shibuya M. A single autophosphorylation site on kdr/flk-1 is essential for vegf-a-dependent activation of plc-gamma and DNA synthesis in vascular endothelial cells. *EMBO J*. 2001;20:2768-2778
22. Chen D, Simons M. Emerging roles of plcgamma1 in endothelial biology. *Sci Signal*. 2021;14
23. Nowotschin S, Xenopoulos P, Schrode N, Hadjantonakis AK. A bright single-cell resolution live imaging reporter of notch signaling in the mouse. *BMC Dev Biol*. 2013;13:15
24. Kholodenko BN, Kolch W, Rukhlenko OS. Reversing pathological cell states: The road less travelled can extend the therapeutic horizon. *Trends Cell Biol*. 2023;33:913-923
25. Rukhlenko OS, Halasz M, Rauch N, Zhernovkov V, Prince T, Wynne K, Maher S, Kashdan E, MacLeod K, Carragher NO, Kolch W, Kholodenko BN. Control of cell state transitions. *Nature*. 2022;609:975-985
26. Yabaji SM, Rukhlenko OS, Chatterjee S, Bhattacharya B, Wood E, Kasaikina M, Kholodenko BN, Gimelbrant AA, Kramnik I. Cell state transition analysis identifies interventions that improve control of mycobacterium tuberculosis infection by susceptible macrophages. *Sci Adv*. 2023;9:eadh4119
27. Suchting S, Freitas C, le Noble F, Benedito R, Breant C, Duarte A, Eichmann A. The notch ligand delta-like 4 negatively regulates endothelial tip cell formation and vessel branching. *Proc Natl Acad Sci U S A*. 2007;104:3225-3230
28. Williams CK, Li JL, Murga M, Harris AL, Tosato G. Up-regulation of the notch ligand delta-like 4 inhibits vegf-induced endothelial cell function. *Blood*. 2006;107:931-939
29. Noguera-Troise I, Daly C, Papadopoulos NJ, Coetzee S, Boland P, Gale NW, Lin HC, Yancopoulos GD, Thurston G. Blockade of dll4 inhibits tumour growth by promoting non-productive angiogenesis. *Nature*. 2006;444:1032-1037
30. Lee HW, Xu Y, He L, Choi W, Gonzalez D, Jin SW, Simons M. Role of venous endothelial cells in developmental and pathologic angiogenesis. *Circulation*. 2021;144:1308-1322
31. Xu C, Hasan SS, Schmidt I, Rocha SF, Pitulescu ME, Bussmann J, Meyen D, Raz E, Adams RH, Siekmann AF. Arteries are formed by vein-derived endothelial tip cells. *Nat Commun*. 2014;5:5758
32. Park H, Furtado J, Poulet M, Chung M, Yun S, Lee S, Sessa WC, Franco CA, Schwartz MA, Eichmann A. Defective flow-migration coupling causes arteriovenous malformations in hereditary hemorrhagic telangiectasia. *Circulation*. 2021;144:805-822
33. Barbacena P, Dominguez-Cejudo M, Fonseca CG, Gomez-Gonzalez M, Faure LM, Zarkada G, Pena A, Pezzarossa A, Ramalho D, Giarratano Y, Ouarne M, Barata D, Fortunato IC, Misikova LH, Mauldin I, Carvalho Y, Trepat X, Roca-Cusachs P, Eichmann A, Bernabeu MO, Franco CA. Competition for endothelial cell polarity drives vascular morphogenesis in the mouse retina. *Dev Cell*. 2022;57:2321-2333 e2329
34. Zhou Y, Williams J, Smallwood PM, Nathans J. Sox7, sox17, and sox18 cooperatively regulate vascular development in the mouse retina. *PLoS One*. 2015;10:e0143650
35. Sanjana NE, Shalem O, Zhang F. Improved vectors and genome-wide libraries for crispr screening. *Nat Methods*. 2014;11:783-784
36. Jostes SV, Fellermeyer M, Arevalo L, Merges GE, Kristiansen G, Nettersheim D, Schorle H. Unique and redundant roles of sox2 and sox17 in regulating the germ cell tumor fate. *Int J Cancer*. 2020;146:1592-1605

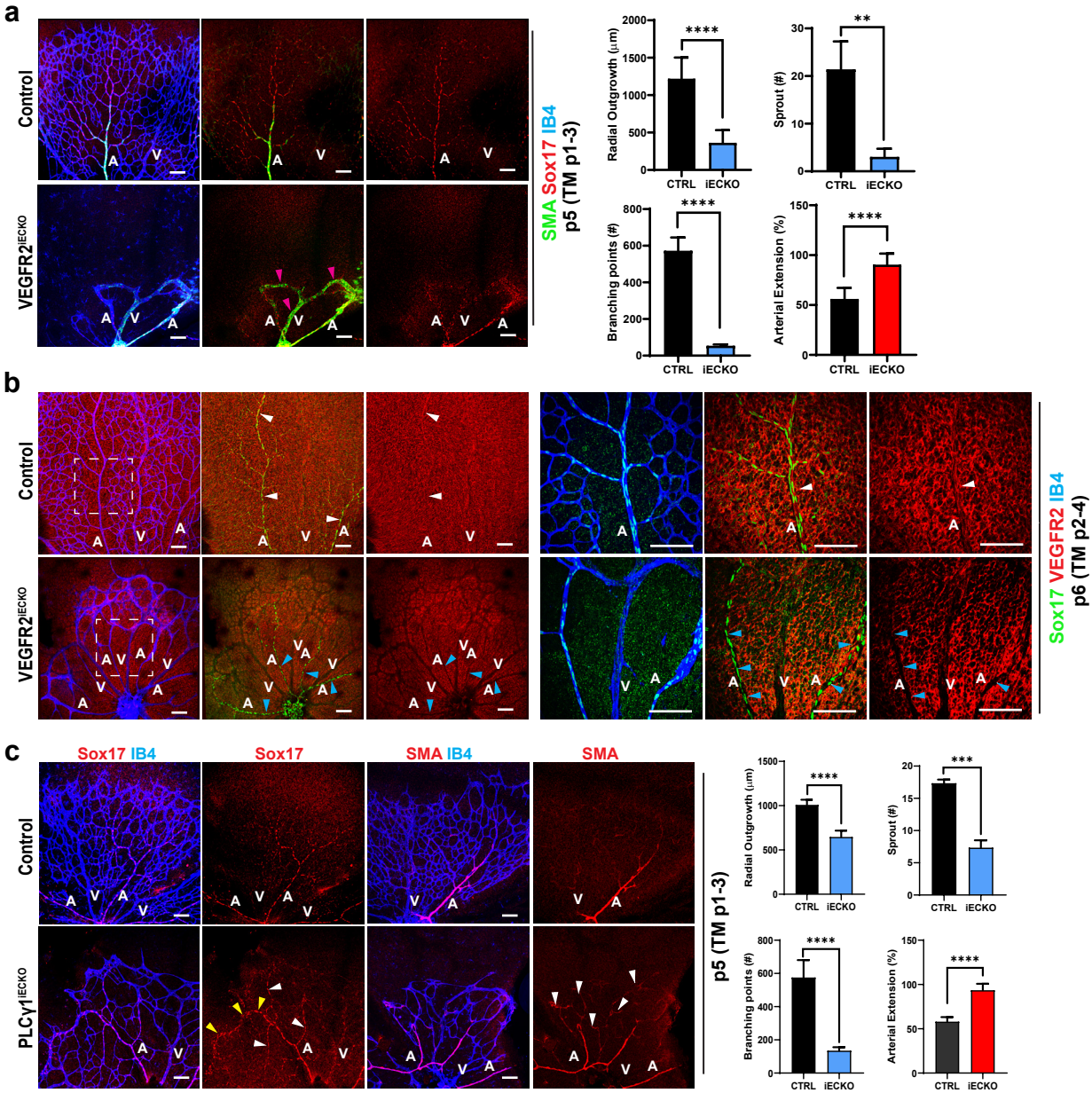

Figure 1: VEGFR2 signaling is not required for arterial fate specification during capillary remodeling.

a. Control and *VEGFR2^{iECKO}* mouse postnatal retinas dissected at p5 (tamoxifen-induced gene deletion at p1-3). Retinas were immunostained with Isolectin B4 (IB4) and antibodies targeting smooth muscle actin (SMA) and Sox17. Pink arrow heads indicate ectopic SMA signal at the vascular front and the vein. Arterial extension is the length of arteries normalized by the diameter of vascular outgrowth. b. Control and *VEGFR2^{iECKO}* mouse postnatal retinas dissected at p6 (tamoxifen-induced gene deletion at p1-3). Retinas were immunostained with IB4 and VEGFR2 to visualize endothelial deletion of VEGFR2. White arrow heads indicate Sox17^{high}/VEGFR2^{+} ECs in the control mice. Blue arrow heads indicate Sox17^{high}/VEGFR2^{null} ECs. c. Control and *PLCγ1^{iECKO}* mouse postnatal retinas dissected at p5 (tamoxifen induction of gene deletion at p1-3). Retinas were immunostained with IB4 and antibodies targeting Sox17 and SMA. Abbreviations: A: artery; V: vein. Scale bars: 100μm.

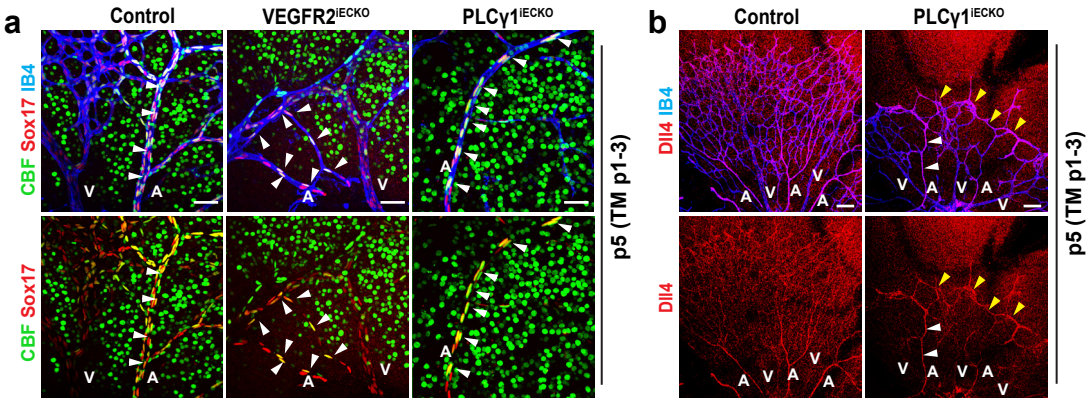

Figure 2: Arterial Notch activation is independent of VEGFR2 signaling.
a. Control, *VEGFR2^{iECKO}* and *PLCγ1^{iECKO}* mice were crossed with Notch reporter line CBF:H2B-Venus to visualize Notch activity. Mouse postnatal retinas dissected at p5 (tamoxifen-induced gene deletion at p1-3) were immunostained with IB4 and Sox17 antibody. Nuclear CBF signal was natural fluorescence from Venus. b. Mouse postnatal retinas from Control and *PLCγ1^{iECKO}* mice were dissected at p5 (tamoxifen induction of gene deletion at p1-3) and immunostained with IB4 and Dll4 antibody.
Abbreviations: A: artery; V: vein. Scale bars: 100μm.

Table1. Vascular phenotypes resulting from defective VEGFR2 signaling

	Sprout	Capillary	Artery
VEGFR2^{iECKO}	Absent	Absent	Arteries formed Sox17^{high}/VEGFR2^{null} ECs Ectopic arterialization at the vascular front and the veins Arterial Notch+
PLCγ1	Few	Reduced	Arteries formed Ectopic arterialization at the vascular front and the veins Arterial Notch+

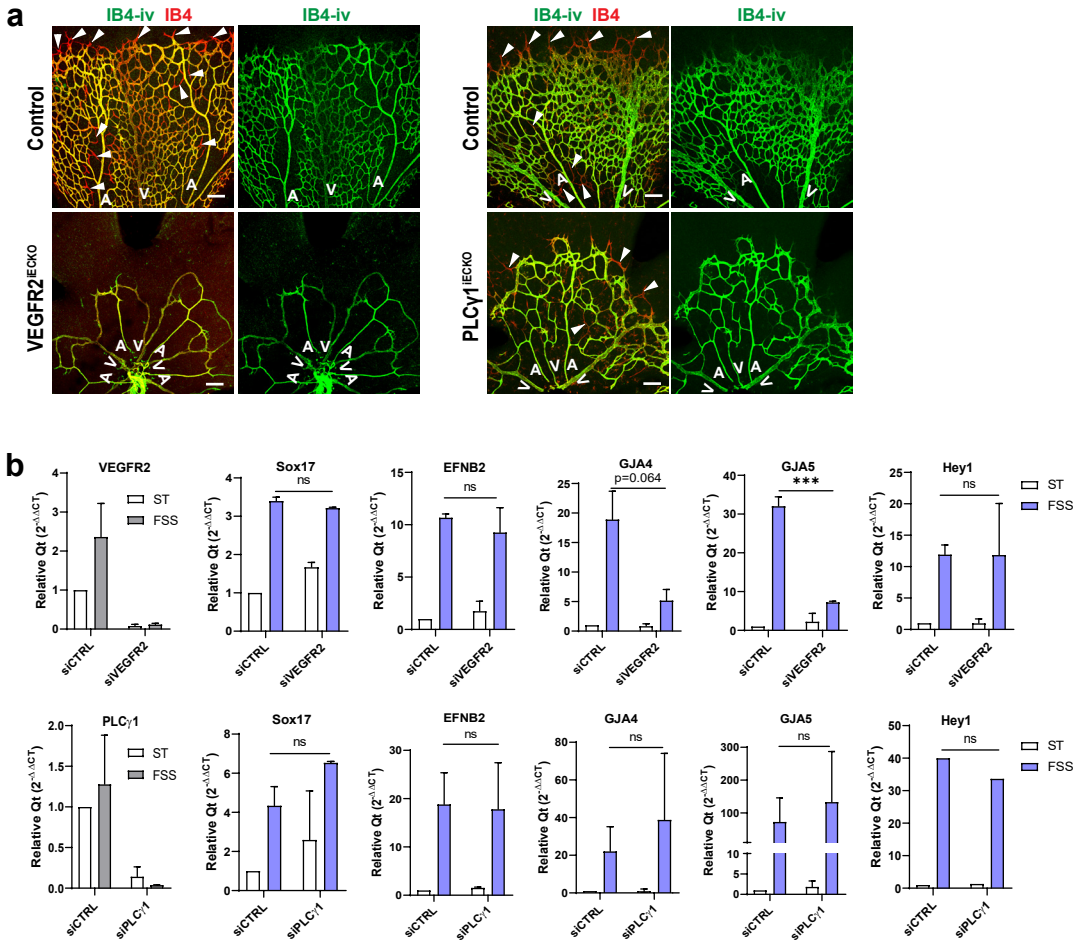

Figure 3: Fluid shear stress-induced arterial specification is independent of VEGFR2 signaling. a. Mouse postnatal retinas were dissected at p5 (tamoxifen-induced gene deletion at p1-3). Before dissection, IB4 (green) was retro-orbitally injected to perfuse the retina vasculatures of Control, *VEGFR2*^{iECKO} and *PLCγ1*^{iECKO} mice. Dissected retinas were stained with IB4 (red) to visualize all perfused and non-perfused blood vessels. Perfused vessels are double-stained (IB4-green/red), while non-perfused vessels were single-stained (IB4-red only, indicated by white arrow heads). Abbreviations: A: artery; V: vein. Scale bars: 100μm. b. HUVECs with siRNA treatments were subjected to static (ST) or FSS (12dyn/cm^2) for 16 hours to induce arterial differentiation. Gene expression was examined by quantitative RT-PCR followed by quantification relative to ST-siCTRL. Student t-test was used for statistics. $p<0.05$ was determined as statistically significant. ns: not significant.

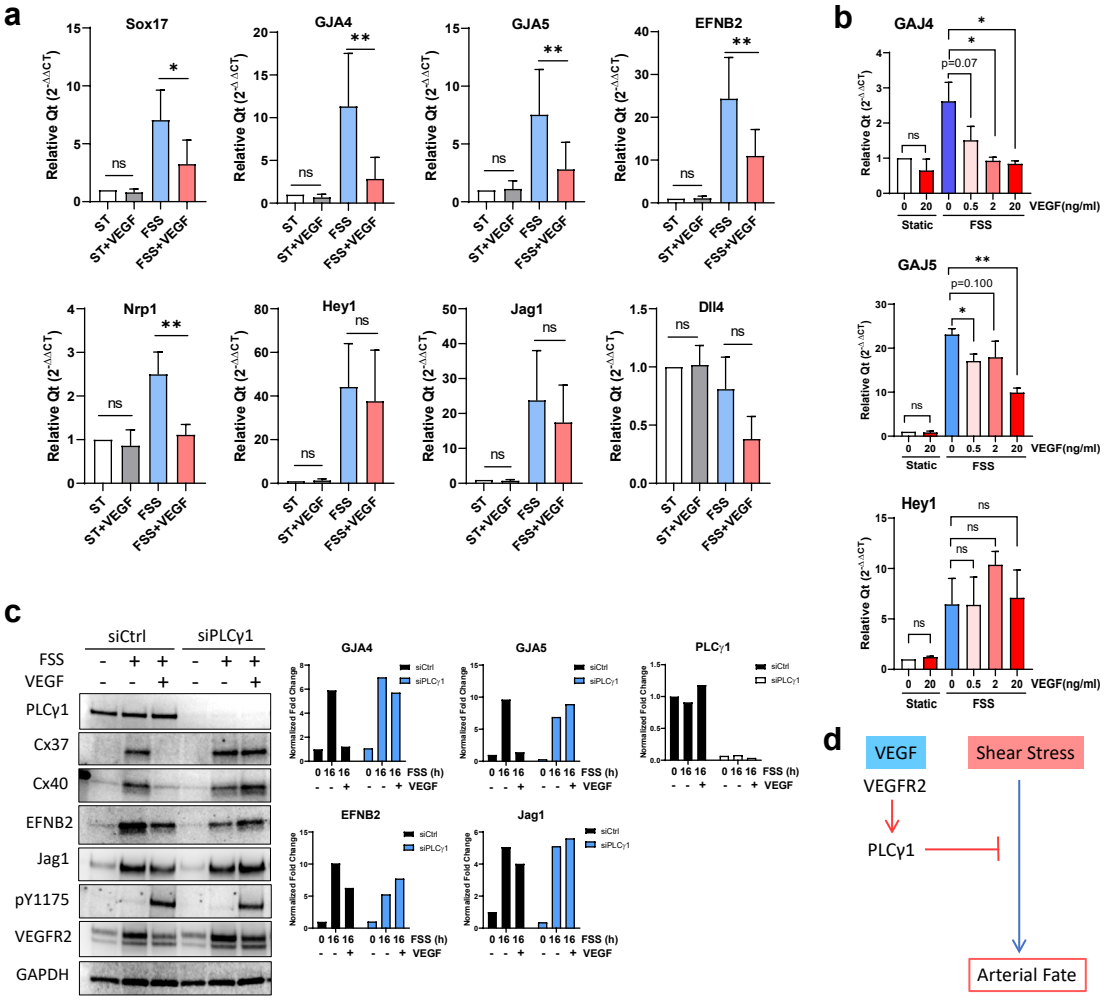

Figure 4. VEGF counteracts FSS-induced arterial specification.

a. HMVBECs were used to test the induction of arterial and Notch genes under the conditions of static (ST), ST with VEGF (20ng/ml), FSS (12dyn/cm^2) and FSS with VEGF. Gene expression was examined by quantitative RT-PCR followed by quantification relative to ST. b. FSS-induced expression of GJA4, GJA5 and Hey1 in HMVBECs with a gradient of VEGF. Gene expression was examined by quantitative RT-PCR followed by quantification relative to ST. FSS experiments were conducted using Vitroflo system. All conditions under FSS were in the same Vitroflo plate. c. HUVECs treated with siRNA were used to test FSS-induced expression of arterial genes and the effect of VEGF. d. A working model demonstrating VEGF signals through VEGFR2-PLCγ1 to counteract FSS-induced arterial specification. Student t-test was used for statistics. $p<0.05$ was determined as statistically significant. ns: not significant.

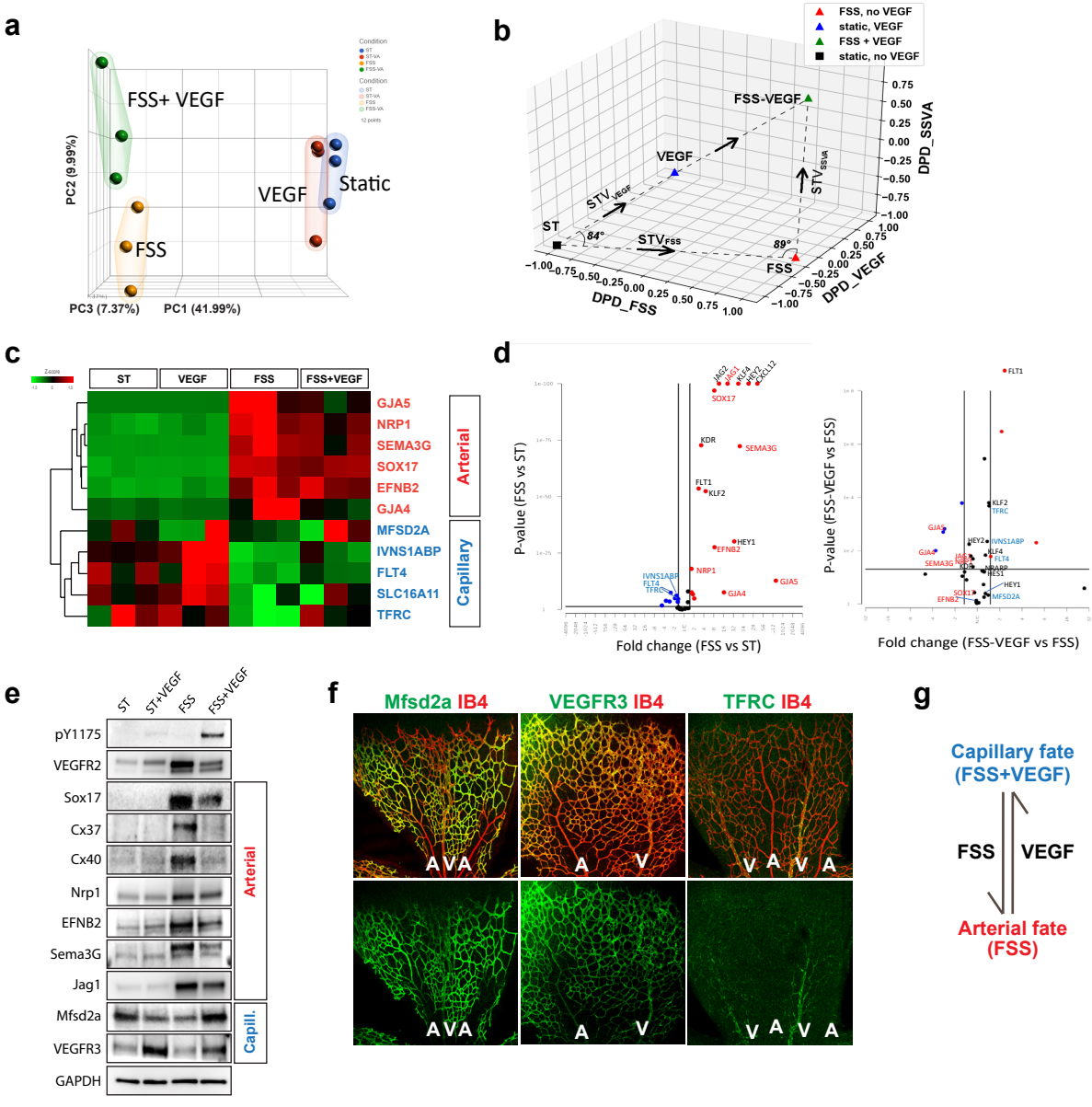

Figure 5. VEGF-FSS competition regulates capillary-to-artery cell fate transition.
a. Principal component analysis (PCA) of RNAseq data. b. cSTAR analysis of RNAseq data. DPD scores of EC states shown in 3D space of the STV_{FSS}, STV_{VEGF}, and STV_{SSVA}. Four EC states correspond to different FSS and VEGF treatments. A change in the EC phenotype is quantified by the DPD score along the corresponding STV. c. Differential gene expression clustered the arterial and capillary genes. d. Volcano plots demonstrating differential expression of the arterial and capillary genes under conditions of FSS versus ST and FSS+VEGF versus FSS, respectively. e. Expression of the arterial and capillary genes examined by wester blots. f. Immunostaining of capillary genes Mfsd2a, VEGFR3 and TFRC in P5 mouse retina. g. A working model: competing signals from VEGF and FSS regulate cell fate transition between capillary and arterial fates.

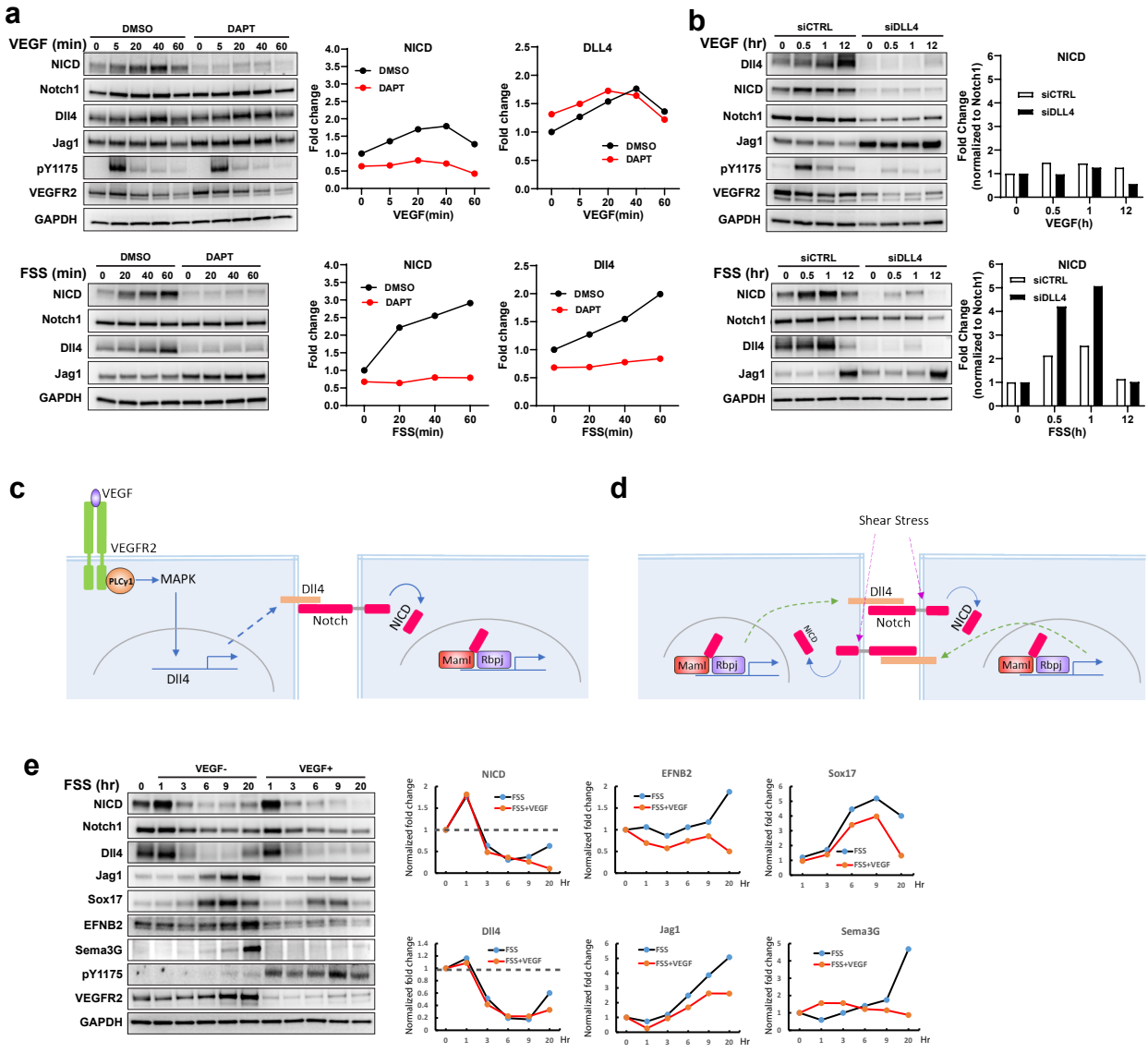

Figure 6. VEGF and shear stress use distinctly different mechanisms to activate Notch.
a. HMVBECs were subjected to VEGF (20ng/ml) or FSS (12 dyn/cm^2) to test the activation of Notch signaling in a time course, with DMSO or γ-secretase inhibitor DAPT treatments. b. HMVBECs treated with siCTRL or siDll4 were subjected to VEGF and FSS to test the activation of Notch signaling. c-d. Working models demonstrating the mechanisms by which VEGF and FSS use to activate Notch signaling. VEGF activates the expression of Dll4, which consequently serves as a ligand to activate Notch signaling in a neighboring cell. By contrast, FSS does not rely on increasing Dll4 expression to activate Notch. Increase of Dll4 expression is a result rather than a cause of FSS-induced Notch activation. e. FSS-induced Notch signaling and expression of arterial genes. HMVBECs were subjected to FSS in a time course in the absence or presence of VEGF.

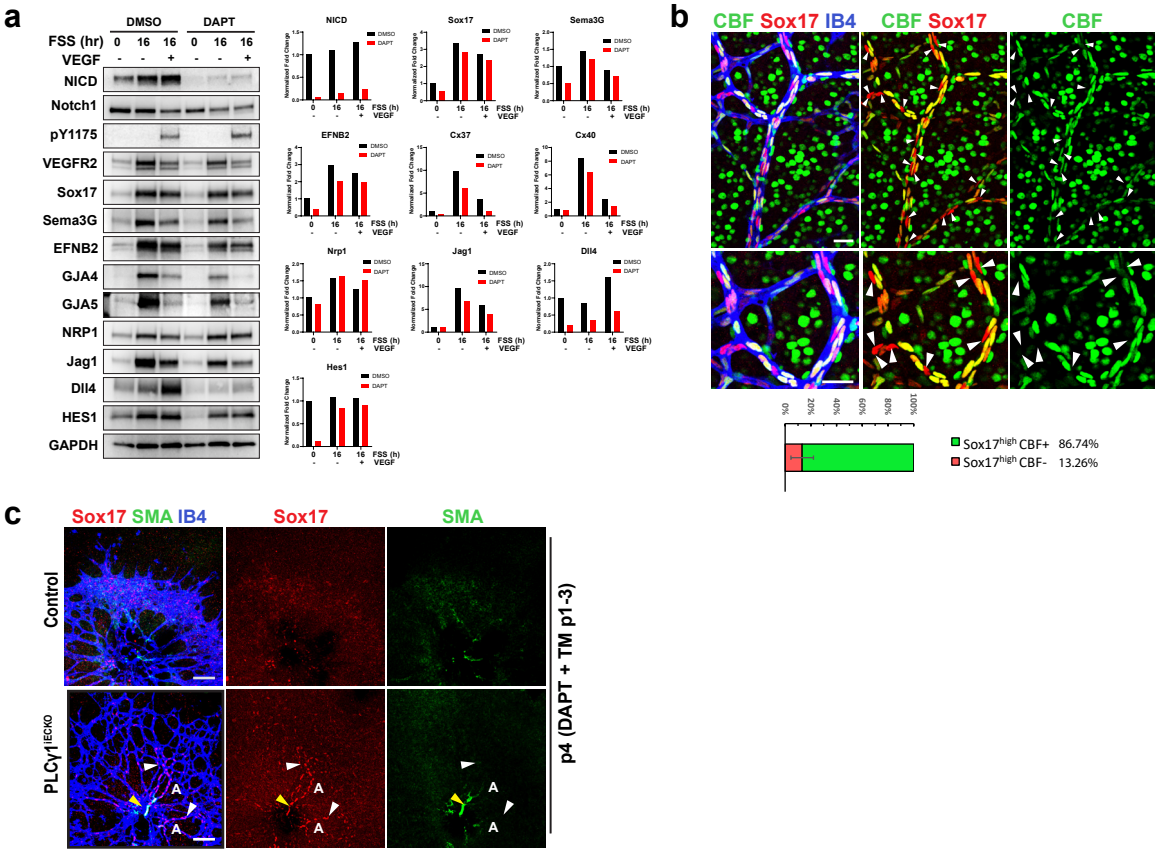

Figure 7. The FSS-arterial program is primarily Notch-independent.

a. Pretreated with DMSO or 5uM DAPT for 3h, HMVBECs were subjected to FSS to induce arterial differentiation for 16h. Samples were analyzed by western blot. b. Representative retinal artery and branching arterioles at p5 from the Notch reporter mouse line CBF:H2B-Venus. Arterial ECs were labeled by immunostaining of Sox17 and colocalized with endogenous Venus signal in the nuclei. Arrow heads indicate Sox17^{high}/CBF- arterial ECs. Scale bars: 25 μm. c. In the background of DAPT-induced Notch inhibition (P1-3), arterial morphogenesis in P4 retina from control and *PLCg1^{iECKO}* mice. White arrow heads indicate arterial morphogenesis marked by Sox17^{high} ECs; yellow arrow heads indicate smooth muscle coverage. Abbreviations: A: artery; V: vein. Scale bars: 100 μm.

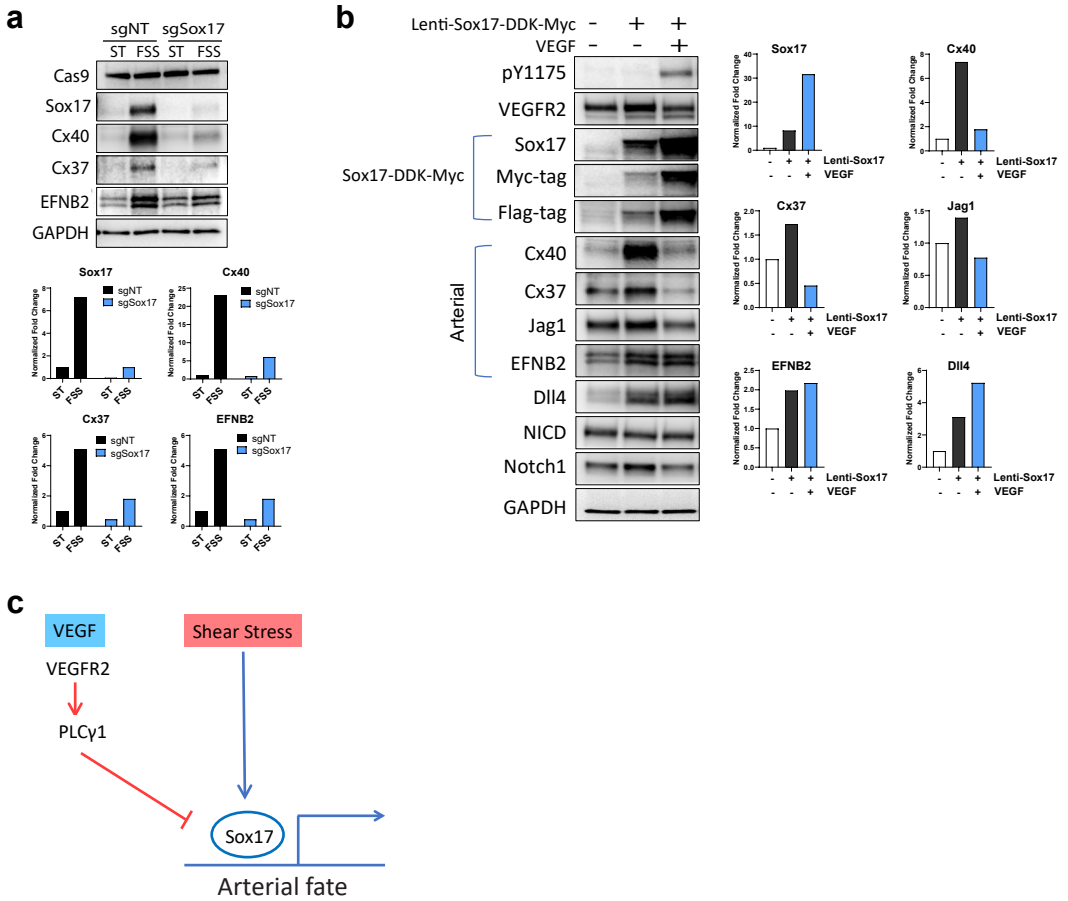

Figure 8. Sox17 is the key to mediate the FSS-arterial program and a target for VEGF-FSS competition.

a. HUVECs with CRISPR-Cas9-directed sgNT or sgSox17 were subject to FSS to induce arterial differentiation. ST: Static. FSS: fluid shear stress. sgNT: non-targeting guide RNA. SgSox17: guide RNA targeting Sox17. b. Western blot of lentivirus-delivered expression of Sox17 dual-tagged with Flag and Myc (Sox17-DDK-Myc) in HUVECs. c. Working model demonstrating the interaction between VEGFR2 signaling and Sox17-mediated FSS-arterial program.

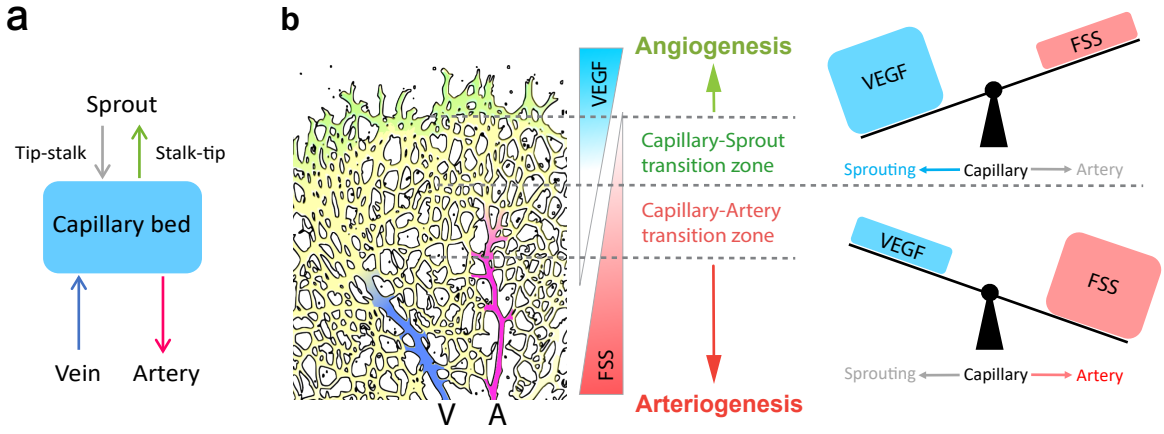

Figure 9. Working model: VEGF and FSS counteract to regulate angiogenesis, capillary maintanance and arteriogenesis.

a. Trajectory of vascular morphogenesis. The whole vasculature originates from the vein, which gives rise to the capillary bed. The capillary bed expands by sprouting angiogenesis towards the peripheral avascular zone, and, at the same time, undergoes a remodeling process to form arteries. b. Gradients of VEGF and FSS counteract to control angiogenesis and arteriogenesis from the capillary bed. The condition with high level of VEGF and low FSS favors angiogenesis and inhibits arteriogenesis, while arteriogenesis requires a decline of VEGF signaling as a permissive prerequisite and high arterial level of FSS to drive arterial specification.